An Overview of Glide Testing

U. V. Nayak, C. K. Lee, T. C. O'Sullivan, J. Hernandez-Fernandez, and D. Gonzalez

***Abstract*—Low flying air-bearings, "sliders," with contact sensors are used to "glide" test magnetic recording disks to be free of asperities above a predetermined height. A technical overview of the considerations necessary for accurate glide testing is illustrated by the example of an experimental flat plate PZT sensor, with electrodes divided into quadrants, to detect asperity contact. The flat plate PZT sensor detects the slider dynamic pitch, roll, and vertical vibrations of the air bearing by contact with asperities of sufficient mechanical stiffness. The sensor also detects contact by the extremely sensitive response of the resonant vibrations of the PZT/slider structure. Different linear combinations of the signal from the quadrants show mode selection based on mode symmetry. The signal response for increasing asperity interference is characterized for specific modes and a mode can be chosen by the appropriate linear combination of the signals from the quadrants. Calibration of the glide slider trailing edge flying height and roll using contact with artificial bumps of different heights is necessary for accurate glide testing. One can map the entire disk surface using the contact signal from both the air-bearing response and the bending mode response simultaneously to identify mechanically "stiff" asperities. Visualization of the mode shapes and characterization the PZT/slider structure using a laser heterodyne interferometer aid in the consistent fabrication of this class of PZT contact sensors. The considerations of sensor response, characterization of the contact signal, techniques to allow consistent PZT/slider fabrication, and calibration methods that allow the signal to be related to the test tolerances represent a technical overview of the requirements for any glide sensor technology.**

***Index Terms*—Air-bearing vibration modes, finite-element modeling, laser heterodyne interferometry, PZT glide heads, shaped PZT electrodes, slider bending modes.**

I. Glide Testing

GLIDE TESTING is used to screen out magnetic recording disks with defects that would make mechanical contact with flying magnetic recording heads. Mechanical contact between recording heads and disk defects have been found to cause data loss due to catastrophic interface failures, accumulation of wear debris/lubricant that cause the magnetic media to be unreadable and unexpected corrosion or degradation of the magnetic recording head. Glide testing requires consideration of the flying response to disk topography of the air bearing used in the magnetic recording file [1]–[4], the contact sensor, signal response, calibration, signal processing, and data acquisition to optimize the information we can gain about disk asperities. Many topographic tools exist that can detect defects on magnetic recording disks. The requirement to be able to detect defects that may be <1 μm in diameter over an area of $\sim$2–5 billion μm^2 and a height of $\sim$5 nm within a few seconds has led to the choice of flying sliders with contact sensors for glide testing. Flying sliders can detect contact across the entire width of the lowest flying trailing edge on the glide slider to scan the magnetic recording disk surface rapidly for defects.

Manuscript received September 2, 2002.

U. V. Nayak is with IBM Research, Almaden Research Center, San Jose, CA 95120 USA (e-mail: nayakuv@almaden.ibm.com).

C. K. Lee is with the National Taiwan University, Taipei, Taiwan.

T. C. O'Sullivan was with IBM Research, Almaden Research Center, San Jose, CA 95120 USA.

J. Hernandez-Fernandez is with Hewlett Packard, Madrid, Spain (e-mail: juan_hernandez@hp.com).

D. Gonzalez is with the Massana Corp., Madrid, Spain.

Digital Object Identifier 10.1109/TMAG.2003.809002

II. Some Asperity Detection Methods

Some methods to detect asperity contact use the pitch, roll, and vertical vibrations of the air bearing of the flying slider to detect disk asperities. The slider-to-disk capacitance [5], [6], small piezoelectric accelerometers [7], [8], or laser-doppler vibrometers [9], [10] are sensitive to sudden slider displacement when asperities have sufficient stiffness to impart a detectable motion in the air bearing.

Other sensors respond indirectly to the contact by using the energy imparted to the mechanical structure. Some examples are the response of resonant structures such as micromechanical cantilevers [11] and "shelves" [12] attached to the slider or "acoustic emission" sensors [13], [14], which respond to asperity contact energy propagated to the suspension or suspension holder.

Other methods to detect disk asperities use some physical property that changes during asperity such as contact temperature or the electrical resistance between slider and disk [15]–[17]. Heated or thermoelectric temperature sensitive elements that respond to either the proximity or physical contact with an asperity are used as "thermal" asperity detectors [18]–[20].

We opted for a piezoelectric sensor that covers the top surface of the slider between the slider and the suspension because, historically, the glide test has to ensure the mechanical reliability of the interface. The piezoelectric sensor (e.g., PZT) signal from this flat plate sensor arises mainly from the compression of the PZT as the sensor accelerates during contact vibrations and from the in-plane stresses of the resonant bending modes of the slider/sensor structure excited during contact. This combination of sensor responses identifies asperities with sufficient stiffness to move the slider at the air-bearing resonant modes and asperities that only excite the slider bending modes. The extremely sensitive signal, shown with less than 0.3 nm of interference (Fig. 1), from the bending modes is obtained if the sensor spans a sufficient area of the vibrating structure. The flat plate sensor will be used to illustrate considerations important, in general, for the use of glide sensors. The data for 100% (4.0 mm $\times$ 3.2 mm $\times$ 0.85 mm) and 62% (2.5 mm $\times$ 1.7 mm $\times$ 0.43 mm) PZT/glide sliders is shown.

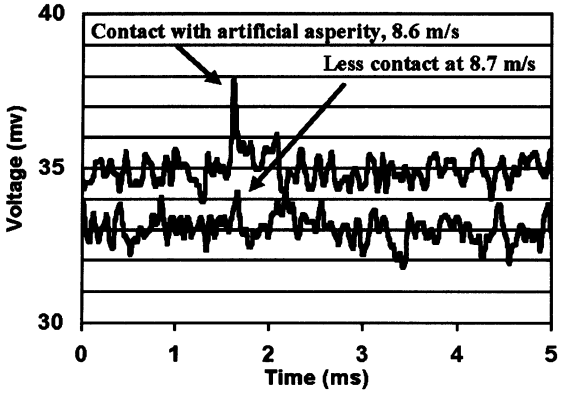

Fig. 1. The envelope of the contact signal with an artificial asperity, 30 nm tall and $\sim 20\,\mu$m in diameter at 8.6 m/s and 8.7 m/s corresponding to a flying height change of 0.3 nm, is shown for the "appropriate" bending modes.

III. The Experimental Quadrant PZT Sensor

To understand the signal from the bending modes we consider the electric displacement of the piezoelectric material, which can be written as [21], [22]

$$D_3 = \varepsilon_{33} E_3 + d_{31}\sigma_x + d_{32}\sigma_y + d_{36}\tau_{xy} \tag{1}$$

where ε denotes the permittivity of the piezoelectric material, σ_x and σ_y are the stresses along the x and y axes, respectively, τ_{xy} is the in-plane shear stress, d is the piezoelectric strain/charge constant, and the subscripts 1$\sim$3 represent x, y, z, and 6 represents xy due to the IEEE compact matrix notation. From Gauss' law, the charge $q(t)$ enclosed by the surface $S^{(12)}$ is

$$q(t) = \int_{S^{(12)}} (\varepsilon_{33} E_3 + d_{31}\sigma_x + d_{32}\sigma_y + d_{36}\tau_{xy})\, dx\, dy. \tag{2}$$

For the piezoelectric material used, PZT-5A, we have

$$d_{31} = d_{32} = d = -171 \times 10^{-12} C/N, \qquad d_{36} = 0. \tag{3}$$

So, (2) can be further reduced to

$$q(t) = d \int_{S^{(12)}} (\sigma_x + \sigma_y)\, dx\, dy \tag{4}$$

where $\sigma_x + \sigma_y$ is an invariant trace of the stress field of a structure for in-plane coordinate transformations. For a flat plate sensor 0.2 mm thick on a 100% slider the signal from the in-plane stress is one order of magnitude larger than the signal from the acceleration of the sensor due to the bending modes.

An experimental PZT sensor was attached to the top surface of the slider with electrodes divided into quadrants (Fig. 2).

Choosing various linear combinations of the signal from the four quadrants allows for mode selection based on their symmetry. The finite element modeling results (Figs. 3, 5, 7, and 9) and the corresponding contact signal (Figs. 4, 6, 8, and 10) obtained by taking different linear combinations of the signals from the quadrants show both mode selection and the observed mode frequencies agree well with the modeling results.

The maximum amplitude of the contact signal was measured for increasing asperity interference by reducing the velocity. Knowing the flying height of the glide slider at different velocities, we can detect the initial "contact height" by bounding

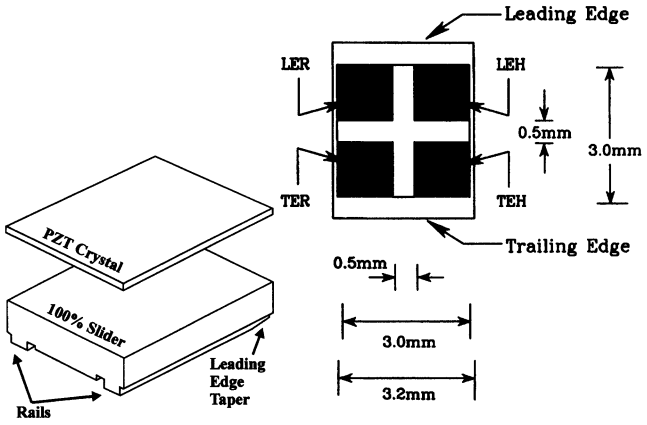

Fig. 2. The flat plate piezoelectric sensor and the sensor surface are shown with the electrodes defined. TE and LE refer to the trailing and leading edges and H and R refer to the hub and rim rail sides.

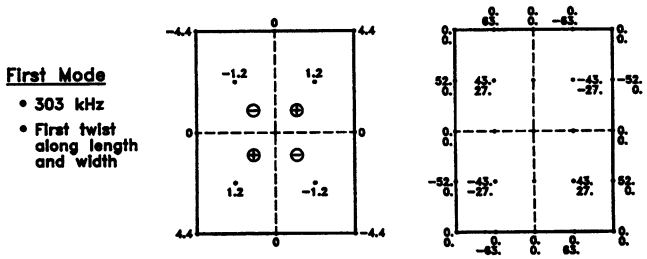

Fig. 3. The relative out-of-plane displacement (left) and the in-plane stress components (right) are shown for the first twist mode of the quadrant PZT on a 100% slider (4.0 mm × 3.2 mm × 0.85 mm) with a 0.2-mm thick PZT5A sensor.

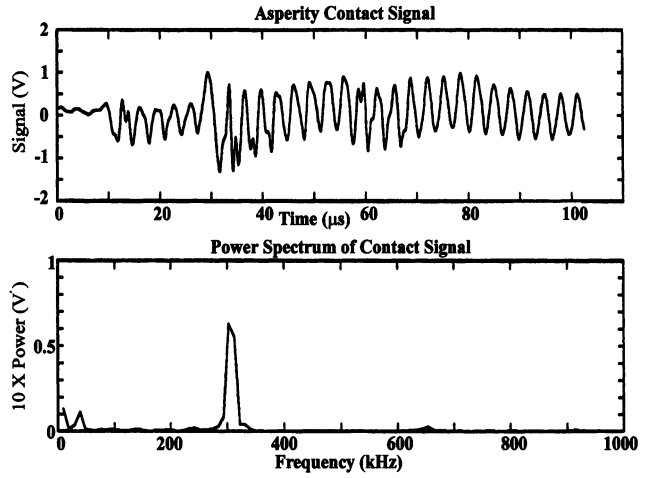

Fig. 4. The contact signal and its power spectrum are for the difference of the diagonal quadrants, (LER + TEH) − (LEH + TER), of the PZT sensor and show the first twist mode.

the "contact velocity" with the asperity to within a narrow velocity range (Fig. 1). The "interference" is the difference between the flying height and the initial contact height. The response to increasing interference can be quite different for the different modes.

To utilize the very sensitive signal from the bending modes, we choose the signal using electrode symmetry of the fifth mode filtered between 1 and 1.5 MHz (fifth mode for the 62% slider) because the response with increasing interference is

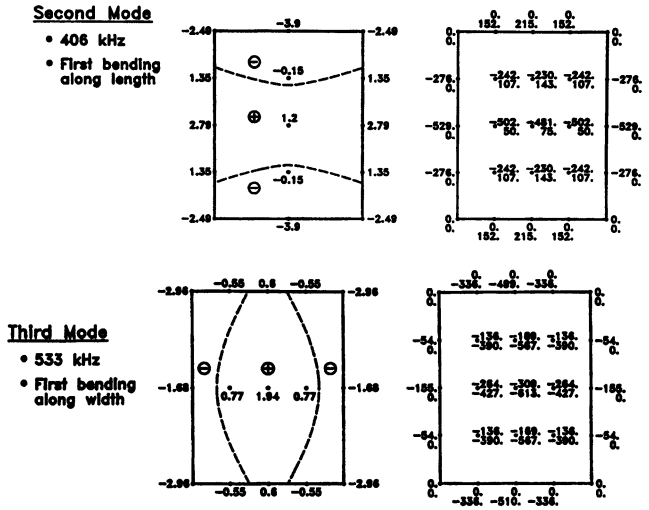

Fig. 5. The relative out-of-plane displacement and the in-plane stress components are shown for the second and third modes, bending along the length and width, respectively, for the quadrant PZT on a 100% slider (4.0 mm × 3.2 mm × 0.85 mm).

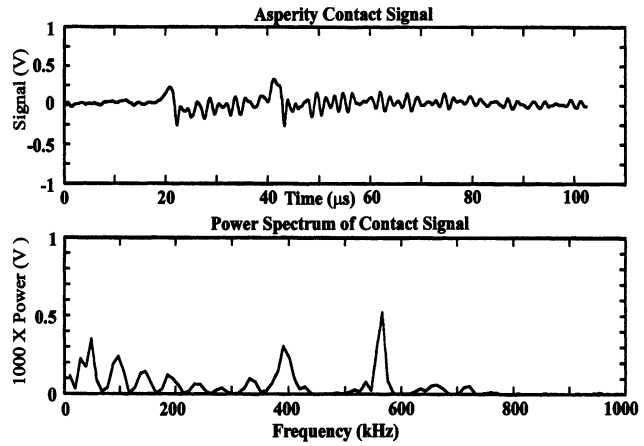

Fig. 6. The contact signal and its power spectrum are for the sum of all the quadrants, LER + LEH + TER + TEH, of the PZT sensor and show the second and third bending modes.

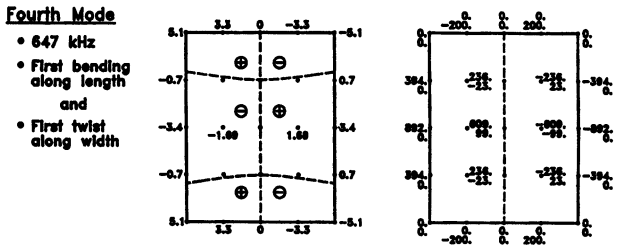

Fig. 7. The relative out of plane displacement and the in-plane stress components are shown for the fourth mode, second twist along the length, of the quadrant PZT on a 100% slider (4.0 mm × 3.2 mm × 0.85 mm).

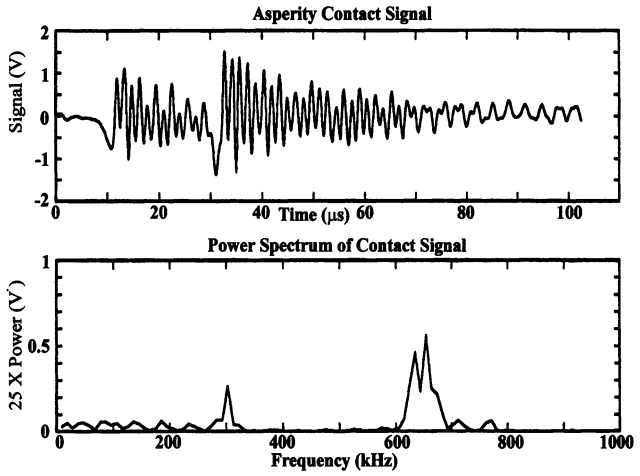

Fig. 8. The contact signal and its power spectrum are for the difference of the rim and hub rail quadrants (LER + TER) − (LEH + TEH) and show the second twist mode along the length.

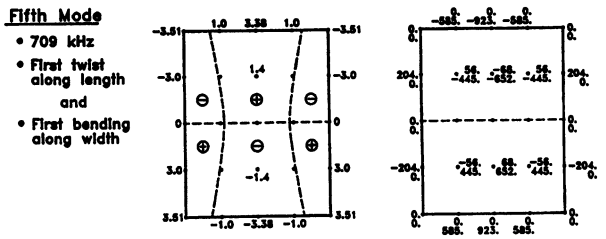

Fig. 9. The relative out-of-plane displacement and the in-plane stress components are shown for the fifth mode, the second twist along the width, for the quadrant PZT on a 100% slider (4.0 mm × 3.2 mm × 0.85 mm).

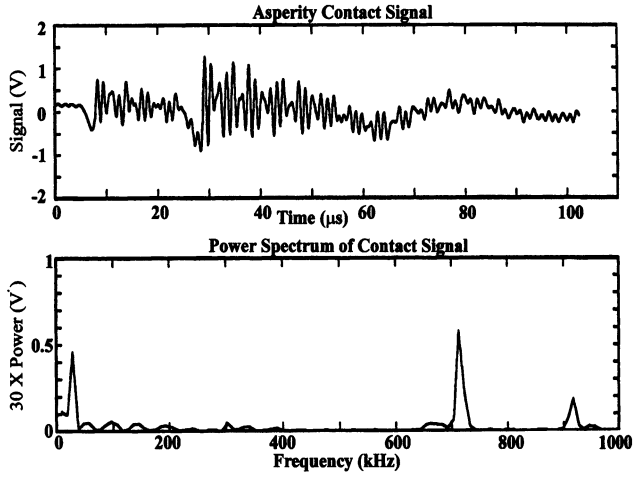

Fig. 10. The contact signal and its power spectrum are for the difference of the leading and trailing edge quadrants (LER + LEH) − (TER + TEH) and show the second twist mode along the width.

more simple (see Fig. 11). The lowest twist mode, selected by taking the signal from the difference of the electrodes along the two diagonals, was found to have a very poor signal-to-noise ratio because it had low damping. The signal from the second and third modes, bending modes along the length and width selected by taking the sum of the signal from all the quadrants, was found to exhibit significant drops in the amplitude even as interference increased (Fig. 11). The fourth mode was not selected because we wished the sensor symmetry to be similar for both side rail and center rail designs of the air bearing used for the glide slider. The contact signal along the center line of the length may result in a very weak contact response for center rail designs for the fourth mode.

The signal, taken simultaneously, from the air-bearing response of the slider to contact with the same asperity is band-pass filtered (20–200 kHz) to include the air-bearing

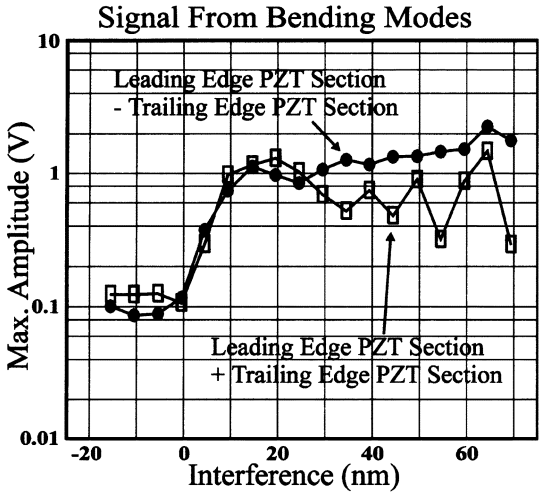

Fig. 11. The maximum amplitude of the contact signal with increasing asperity interference, by reducing disk speed for a 62% slider with a center rail design, was used to choose signal response desirable for glide testing. The artificial asperity used is 90 nm tall and ~20 μm in diameter. The plot shows the signal from two different linear combinations of the signal from the electrodes of the sensor sensitive to different slider/sensor bending modes. A similar effect is seen for the 100% slider with the quadrant electrode.

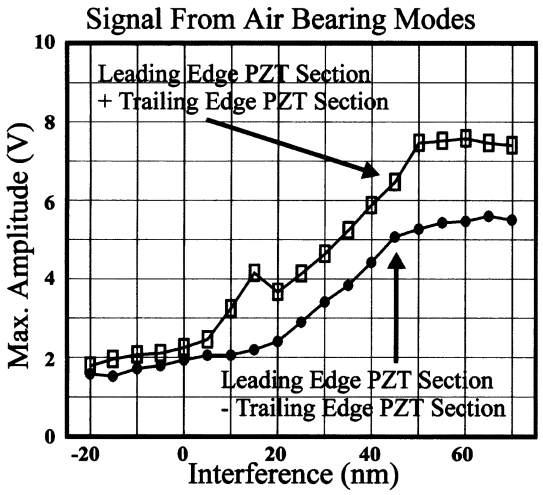

Fig. 12. The maximum amplitude (20–200 kHz) of the contact signal from the air-bearing modes with increasing asperity interference for a 62% slider used to choose signal response desirable for glide testing.

modes of the glide slider shown in Fig. 12. The amplitude response for increasing interference shows that by choosing the difference of the signal from the leading edge and trailing edge electrodes, we can use simple amplitude threshold contact detection for glide testing for both the air-bearing modes and the bending modes. This linear combination is more immune to pickup of extraneous signals.

IV. Bump Contact Calibration

Because of the high sensitivity of the slider bending modes to contact (Fig. 1), we can do *in situ* calibration of the glide slider. We can detect the velocity of contact with artificial bumps with different heights made on a special calibration disk by the slider trailing edge (TE) for flying height, the TE roll, TE camber, and

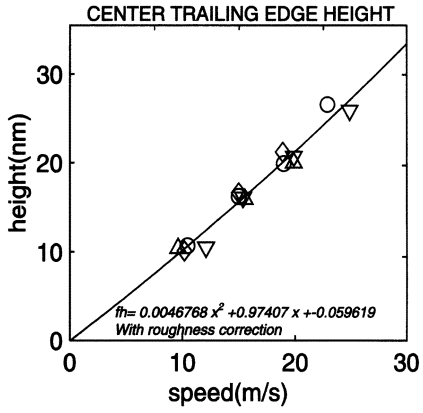

Fig. 13. Contact velocity with bumps of different heights on a calibration disk.

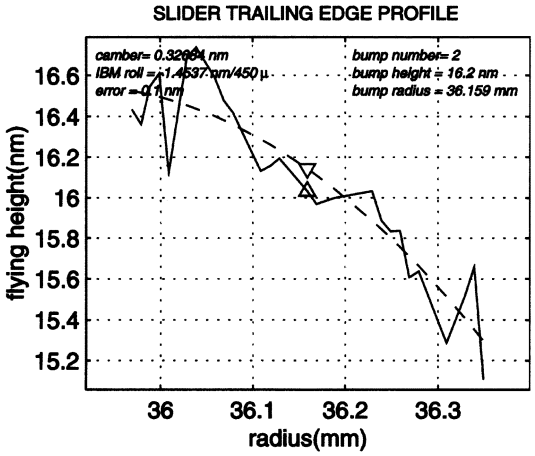

Fig. 14. Contact velocity is converted into flying height for different positions along the slider trailing edge using the data from Fig. 13. The plot shows the trailing edge flying height fit to a parabola.

TE roughness by detecting the velocity of contact. The bumps made for calibration have to be small enough (~17 μm diameter) so that the slider spacing is not affected significantly by the increased air-bearing pressure across the bump. The slider is flown with a few nanometers of interference with a bump of a calibrated height, scanned radially across the bump to detect the slider rail edges, positioned at the center of trailing edge (CTE) and then contact velocity with the bump is determined. Following this procedure for bumps of different heights gives us the bump height and the corresponding bump contact velocities (Fig. 13). Moving the slider radially across the bump and determining the contact velocity at various points along the slider trailing edge gives us a radial contact velocity profile. Using the velocity to height data from Fig. 13, we get the flying height "rail profile" across the trailing edge (Fig. 14). Fitting this flying height "rail profile" data to a parabola we can extract the roll and the camber of the trailing edge of the slider used for asperity detection in glide. The residuals from the fit give us the "roughness" of the slider trailing edge (Fig. 15). The use of such an *in situ* calibration method significantly improves the accuracy of glide test because we can couple very high contact sensitivity with very well-characterized slider trailing edge that makes contact with the asperities.

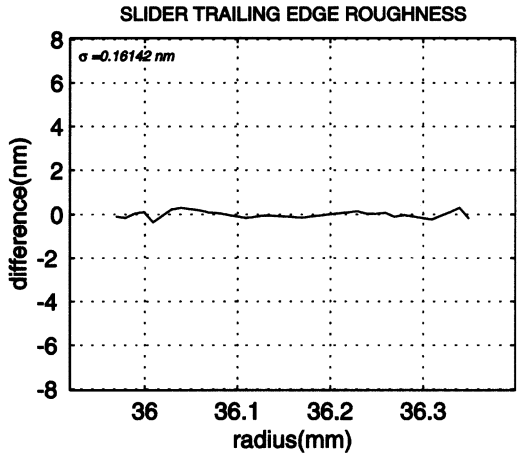

Fig. 15. Residuals from the fit to the trailing edge flying height in Fig. 14. This is the "roughness" of the trailing edge.

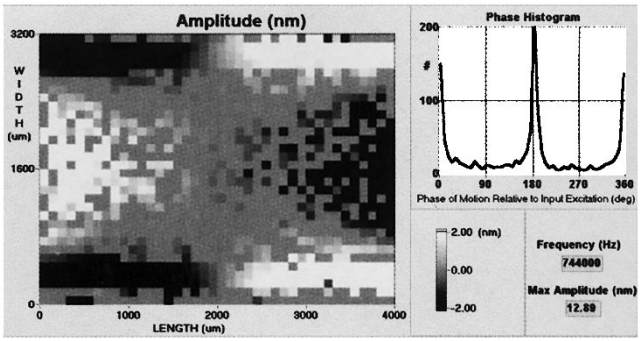

Fig. 16. Displacement of the fifth mode across the surface of the slider is excited by applying an oscillatory potential at the resonant frequency (744 kHz) to the leading edge quadrants. The motion is characterized by regions of 0 deg phase (white) and 180 deg phase (black) as seen in the phase histogram.

V. Sensor Characterization Technologies for Fabrication

The accuracy of the glide test also depends on the quality of the glide sensor and the consistency of fabrication methods. We can measure the properties of the PZT/slider structure using the PZT sensor as an actuator. By applying a signal at the resonant frequency of individual modes to appropriate electrodes of the quadrant PZT sensor we can make the structure vibrate at its resonant modes. We can visualize the mode shape and the efficiency of excitation of that mode using laser heterodyne interferometery [23]–[25]. For example, the mode shape of the fifth mode (Fig. 9) of the 100% slider with the quadrant PZT is excited by applying a signal from an oscillator to the leading edge electrodes at the resonant frequency (744 kHz) for that PZT/slider. We can discriminate the phase of the displacement by triggering the capture of the I (0 deg) and Q (90 deg) phases from the heterodyne interferometer synchronously with the oscillator signal. Decoding the signal gives us the relative phase and amplitude of the motion of PZT/slider structure measured at different spots on the "air-bearing" side of the slider at 100-μm intervals to construct the mode shape (Fig. 16).

The quadrant PZT/slider can also be excited by a tone burst at the resonant frequency of a mode applied to the leading edge quadrants (Fig. 17). A sufficiently long tone burst causes the displacement to reach a steady amplitude and the displacement decays exponentially after the burst is turned off. After "envelope" detection of the amplitude of the displacement signal analytically, the data of the exponentially decaying amplitude is fit to get the damping time constant. The amplitude, damping, and the absence of mode mixing are qualitative measures of the quality of the fabrication of the PZT glide sensor.

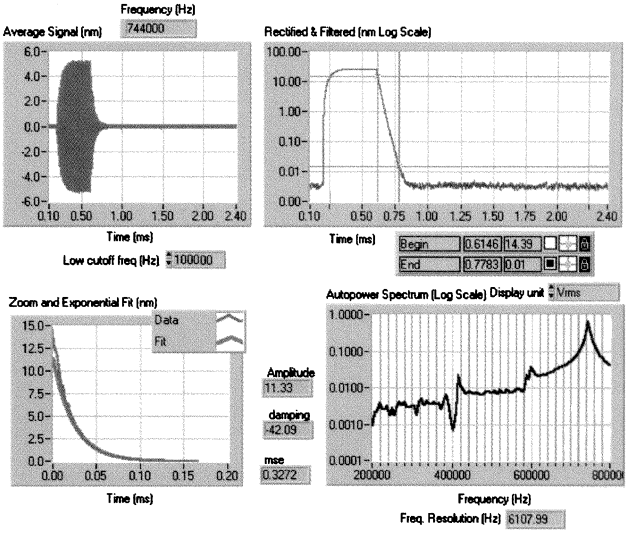

Fig. 17. Displacement at an antinode of the fifth mode is excited by applying a tone burst at the resonant frequency (744 kHz). The exponential damping of the fifth mode is seen as the displacement amplitude diminishes after the tone burst is turned off. The spectrum shows the amplitude of other modes that are excited (i.e., mode mixing).

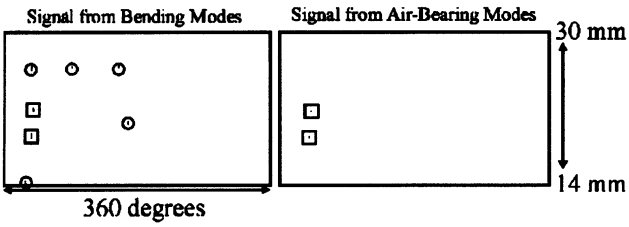

Fig. 18. The asperity map of a 65-mm diameter disk surface at a flying height of 8 nm using the signal from the slider bending modes and the signal from the slider air-bearing modes using a 62% slider. The boxes highlight contacts seen in both modes and the circles show asperities seen only in the signal from the bending modes.

VI. Use of PZT Modal Sensors for Disk Asperity Characterization (Disk Mapping)

With all the conditions of sensitivity, choice of modes with appropriate sensor response, calibration of slider TE flying height state, and consistent sensor response we are now ready to measure the asperity distribution on the disk. The asperity mapping (Fig. 18) is performed using dual contact detection channels that simultaneously measure the signal from the dynamic response of the air bearing to contact (stiff asperities) and asperities that are too small to "move" the slider. The measurements are performed at constant flying height (i.e., constant velocity) as the slider traverses radially across the disk surface. We can see the maps help us identify asperities with great sensitivity as well as the asperities with higher stiffness.

Performing these maps at different flying heights gives us valuable information about the asperity distribution with height, asperity spatial localization, and asperity characteristics.

VII. Summary

The flat plate piezoelectric glide sensor illustrates issues that need to be addressed to perform an accurate glide test with any glide technology. We need the following:

- a glide air-bearing that flies with a response to the disk similar to product sliders;
- a highly sensitive contact response that is understood theoretically for appropriate sensor design;
- to understand signal response to asperities of differing mechanical properties;
- a sensor contact response that simplifies signal processing;
- calibration methods to link the sensor response to flying height and asperity interference heights;
- data acquisition methods that extract and display the information from the sensor signal during glide test;
- methods to characterize and fabricate these sensors consistently with these characteristics.

The flat plate PZT sensor technology used to illustrate these requirements is a technology that can be extended to current and future product slider aspect ratios and air-bearing technologies.

References

[1] S. Fukui, K. Kogure, and Y. Mitsuya, "Dynamic characteristics of flying head sliders on running wavy disk," in *Tribology and Mechanics of Magnetic Storage Systems*: Amer. Soc. Lubrication Engineers, 1985, SP-19.

[2] M. Suk, B. Bhushan, and D. B. Bogy, "Role of disk surface roughness on slider flying height and air-bearing frequency," *IEEE Trans. Magn.*, vol. 26, p. 2493, 1990.

[3] S. Suzuki and H. Nishihira, "Study of slider dynamics over very smooth magnetic disks," *J. Tribology*, vol. 118, p. 382, 1996.

[4] D. Gonzalez, V. Nayak, B. Marchon, R. Payne, D. Crump, and P. Dennig, "The dynamic coupling of the slider to the disk surface and its relevance to take off height," *IEEE Trans. Magn.*, vol. 37, pp. 1839–1841, July 2001.

[5] C. Lin, "Optimum gain of capacitance slider," *IBM Tech. Discl. Bull.*, vol. 21, no. 12, pp. 4996–4998, May 1979.

[6] G. L. Best, "Comparison of optical and capacitive measurements of slider dynamics," *IEEE Trans. Magn.*, vol. MAG–23, p. 3453, Sept. 1987.

[7] C. E. Yeack-Scranton and S. F. Vogel, "Apparatus for analyzing the interface between a recording disk and a read-write head," U.S. Patent 4 532 802, Aug. 6, 1985.

[8] C. E. Yeack-Scranton, "Novel piezoelectric transducer to monitor head-disk interactions," *IEEE Trans. Magn.*, vol. MAG–22, p. 1011, Sept. 1986.

[9] L.-Y. Zhu and D. B. Bogy, "A comparison of head-to-disk spacing fluctuation and hard stretch-surface recording disks," *IEEE Trans. Magn.*, vol. MAG–23, p. 3447, Sept. 1987.

[10] D. W. Meyer, T. Schar, and G. J. Smith, "Glide testing using a laser-Doppler vibrometer/interferometer," *IBM Tech. Discl. Bull.*, vol. 37, no. 10, pp. 367–368, 1994.

[11] K. E. Petersen, A. Shartel, and N. F. Raley, "Micromechanical accelerometer integrated with MOS detection circuitry," *IEEE Trans. Electron. Devices*, vol. 29, pp. 23–27, Jan. 1982.

[12] A. Y. Tsay, R. C. Ku, I. Y. Shen, and B. Marchon, *Natural Frequency Analysis of PZT Glide Heads During Contact*: ASME ISPS, 1998, vol. 4, pp. 91–96.

[13] T. Kita, K. Kogure, Y. Mitsuya, and T. Nakanishi, "New method of detecting contact between floating head and disk," *IEEE Trans. Magn.*, vol. MAG–16, p. 873, Sept. 1980.

[14] R. C. Tseng and G. O. Zierdt, "A glide test to assure disk surface quality," *IBM Disk Storage Technol.*, Feb. 1980.

[15] R. C. Tseng and F. E. Talke, "Transition from boundary lubrication of slider bearings," *IBM J. Res. Dev.*, vol. 18, no. 6, pp. 534–540, 1974.

[16] J. Kishigami, T. Ohkubo, and Y. Koshimoto, "An experimental investigation of contact characteristics between a slider and medium using the electrical resistance method," *IEEE Trans. Magn.*, vol. 26, pp. 2205–2207, Sept. 1990.

[17] T. G. Jeong and D. B. Bogy, "Use of the electrical resistance method to detect slider-disk contacts during contact-start-stop and dynamic load-unload," in *Advances in Information Storage Systems*. New York: ASME Press, 1992, vol. 4, pp. 195–207.

[18] G. N. Nelson, F. E. Talke, and R. C. Tseng, "Magnetoresistive sensing of surface burnishing," *IBM Tech. Disc. Bull.*, vol. 6, p. 243, 1975.

[19] R. Sundaram, Y. Wei, R. C. Ku, and D. Kuo, "Study of head/disc interface dynamics using a thermal asperity sensor," *IEEE Trans. Magn.*, pt. 1, vol. 35, pp. 2481–2483, Sept. 1999.

[20] M. Boyd and X. Xiaopeng, "MR glide inspection for hard disk defect detection," in *Proc. SPIE-Int. Soc. Opt. Eng.*, vol. 3619, USA, 1999, pp. 53–64.

[21] C.-K. Lee, "Piezoelectric laminates for torsional and bending modal control: Theory and experiment," Ph.D. dissertation, Cornell Univ., Ithaca, NY, 1987.

[22] ANSI/IEEE Standard 176, "Piezoelectricity," IEEE, New York, 1987.

[23] *Precision Optical Displacement Sensor (PODS)*. Pointe Claire, QC, Canada: MPB Technologies Inc..

[24] J. H. Ou-Yang, A. Y. Tsay, I. Y. Shen, and D. Kuo, "Experimental and theoretical studies of PZT glide head vibration," *IEEE Trans. Magn.*, pt. 1, vol. 35, pp. 2493–2495, Sept. 1999.

[25] J. Hernández-Fernández, "Sistema de control de un interferómetro láser para caracterización de la superficie de discos duros," Masters project, ETSI, Madrid, Spain, 2001.